Clinics of Surgery[R]

ISSN 2689-8268 Volume 11

Research Article Open Access

Pathology Foundation Models to Reveal Prognostic Features and Molecular Correlations in Head and Neck Squamous Cell Carcinoma

Pil-Jong Kim*

Dental Multiomics Center, School of Dentistry and Dental Research Institute, Seoul National University, Seoul, Republic of Korea

***Corresponding author:**

Pil-Jong Kim, DDS, PhD,
School of Dentistry, Seoul National University#402, Dentistry Graduate School of Seoul National University, 1, Gwanak-ro, Gwanak-gu, Seoul, Republic of Korea
ORCID: 0000-0001-8544-7909

Received: 03 Aug 2025
Accepted: 29 Aug 2025
Published: 06 Sep 2025
J Short Name: COS

Keywords:

Head and Neck Squamous Cell Carcinoma; Pathology Foundation Model; Gene Ontology; mRNA Expression; Personalized Treatment

Citation:

Pil-Jong Kim, Pathology Foundation Models to Reveal Prognostic Features and Molecular Correlations in Head and Neck Squamous Cell Carcinoma. Clinics of Surgery® 2025; V11(1): 1-9

1. Abstract

1.1. Aims

Head and neck squamous cell carcinoma (HNSC) diagnosis is complicated by tumor heterogeneity and subjective evaluation. This study aimed to evaluate whether AI-driven pathology foundation models trained on diverse whole-slide images (WSIs) can provide prognostic features that improve diagnostic accuracy, reduce inter-observer variability, and ultimately enhance patient outcomes.

1.2. Methods

WSIs, clinical, and mRNA expression data for HNSC were obtained from The Cancer Genome Atlas (TCGA) and Clinical Proteomic Tumor Analysis Consortium (CPTAC). Three pathology foundation models (PRISM, Prov-GigaPath, and MADELEINE) were applied to extract features from each WSI. Stepwise variable selection in Cox proportional hazards models was performed, and prognostically significant features were identified using the lowest p-value cutoff. Spearman's correlation (≥0.3) linked features to mRNA expression, followed by Gene Ontology Biological Process (GO-BP) enrichment with false discovery rate (FDR) correction.

1.3. Results

A total of 589 cases (447 TCGA, 142 CPTAC) showed comparable survival distributions. Across models, 10–11% of extracted features were highly inter-correlated. A smaller subset (0.89–2.09%) demonstrated strong correlations with mRNA expression, repeatedly highlighting genes such as PXYLP1 and BCL10. GO enrichment revealed biologically relevant processes including epidermis development and keratinocyte differentiation, underscoring the clinical significance of these AI-derived features.

1.4. Conclusion

Pathology foundation models demonstrate strong potential in identifying prognostic morphological features in HNSC. Despite variability across cohorts and models, these approaches show promise for improving diagnostic precision and advancing patient care through earlier and more accurate prognostication.

2. Introduction

Its incidence varies across regions, strongly influenced by tobacco and alcohol use as well as human papillomavirus (HPV) infection, which adds to the epidemiological complexity of the disease [1]. Its incidence varies across regions, strongly influenced by tobacco and alcohol use as well as human papillomavirus (HPV) infection, which adds to the epidemiological complexity of the disease [2]. Despite advances in surgery, radiotherapy, chemotherapy, and targeted therapy, prognosis for advanced HNSC remains poor. Histopathological examination remains the diagnostic gold standard [3]. A major challenge lies in the marked heterogeneity of HNSC. Individual tumors often exhibit diverse differentiation patterns, ranging from well- to poorly differentiated cells, and are embedded in a complex tumor microenvironment (TME) comprising immune, stromal, and vascular elements [4]. This morphological diversity contributes to interpretive variability, with outcomes influenced by both the subjectivity of microscopy-based assessments and inter-observer differences [5]. Recent computational approaches aim to mitigate these challenges by reducing variability and standardizing evaluations. The digitization of whole-slide images (WSIs) has enabled the integration of

artificial intelligence (AI) and machine learning (ML) into pathology. Deep learning-particularly Convolutional Neural Networks (CNNs)-has transformed image analysis by learning discriminative features directly from large datasets [6]. In pathology, CNNs have already demonstrated success in mitotic figure detection, tumor segmentation, and tissue classification [7]. Uilding on this, the concept of foundation models has emerged [9]. These are large-scale neural networks trained on diverse WSI collections across cancer types, staining protocols, and institutions. Exposure to such variation allows the models to learn broadly representative morphological patterns, which can then be transferred to new tasks through fine-tuning [9]. Their strength lies in leveraging generalized histological knowledge, thereby improving adaptability and efficiency for downstream clinical and research applications. In HNSC, pathology foundation models offer distinct advantages. First, they analyze entire WSIs rather than limited regions of interest, ensuring that subtle but clinically important features-such as stromal invasion at tumor boundaries-are not overlooked [10]. Second, they can detect patterns beyond human perception, including early perineural invasion or nuanced stromal alterations [11]. Third, by producing objective and reproducible outputs, these models have the potential to minimize inter-observer variability and accelerate diagnostic workflows [12]. Collectively, these capabilities may enable faster, more accurate diagnoses and more reliable clinical decision-making. Clinically, the ability to identify and quantify histopathological features at scale has far-reaching implications. Detecting occult stromal invasion or early perineural infiltration could influence surgical margins and decisions regarding adjuvant therapy [13]. Quantifying tumor-infiltrating lymphocytes may help predict immunotherapy response, particularly in HPV-associated oropharyngeal cancers [14]. Beyond individual patient care, large-scale computational analyses of WSIs can deepen understanding of the HNSC TME, revealing spatial immune or stromal patterns associated with prognosis and treatment response [15]. Such insights are difficult to achieve through manual review alone but are well suited to AI-driven analysis. Through a systematic evaluation of multiple publicly available datasets, we aim to demonstrate how pathology foundation models can enhance diagnostic accuracy, reduce variability, and provide biologically meaningful insights-advancing both clinical management and translational research in head and neck oncology.

3. Materials & Methods

3.1. Data Acquisition

Whole-slide images (WSIs) of head and neck squamous cell carcinoma (HNSC) were obtained from two publicly accessible repositories: The Cancer Genome Atlas (TCGA) and the Clinical Proteomic Tumor Analysis Consortium (CPTAC). TCGA-HNSC data were downloaded through the Genomic Data Commons (GDC) portal (https://portal.gdc.cancer.gov/), while CPTAC-HNSC datasets were accessed via the CPTAC Data Portal (https://proteomics.cancer.gov/data-portal/). Searches were conducted using the keyword HNSC, and filters were applied to isolate diagnostic WSIs in standard formats (e.g., SVS). Patient-level clinical information, including overall survival (OS) time and survival status, was linked to the corresponding WSIs using patient identifiers. These clinical data were harmonized across cohorts for integrated survival analyses. Additionally, mRNA expression profiles associated with each case were retrieved and merged with the histopathology data to facilitate multimodal analyses.

3.2. Slide Feature Extraction Model Setup

The overall workflow of the study is summarized in Figure 1. Three pathology foundation models-PRISM, Prov-Giga Path, and MADELEINE-were employed for feature extraction [6-18]. The models of PRISM, Prov-Giga Path, and MADELEINE were obtained in https://huggingface.co/paige-ai/Prism, https://huggingface.co/prov-gigapath/prov-gigapath and https://github.com/mahmoodlab/MADELEINE, respectively. For PRISM and Prov-Giga Path, WSIs were segmented into smaller non-overlapping patches at the required magnification using a custom Python script based on the Open Slide library. MADELEINE incorporates an end-to-end pipeline that processes entire WSIs directly to generate feature vectors. All extracted features were stored in a structured tabular format for downstream survival and bioinformatics analyses.

3.3. Slide Analysis Based on Survival Analysis

Prognostic evaluation of the WSI-derived features was performed using the Cox proportional hazards regression model. Initially, each feature was subjected to univariable Cox analysis to assess its association with overall survival. Harrell's concordance index (c-index) was calculated for each feature as a continuous variable, and the results were corrected using a 1,000-trial bootstrap procedure to provide a robust estimate of predictive performance. To further examine clinical relevance, a “best p-value cutoff” strategy was implemented [19]. For each feature, multiple candidate cutoff values were tested, and the threshold that produced the most statistically significant separation in overall survival was selected. This data-driven approach was chosen over conventional cutoffs, such as the median or mean, in order to account for nonlinear or skewed distributions. To avoid artificially small subgroups, a minimum group size of 10% of the cohort was required when determining cutoffs. Patients were then stratified according to the optimal cutoff for each feature, and Kaplan–Meier survival curves were generated to illustrate differences in overall survival between groups. Together, these analyses allowed us to identify foundation model-derived features with significant and reproducible prognostic value in HNSC.

3.4. Functional Enrichment Analysis and Statistical Analysis

To explore the biological significance of prognostic features, Spearman's correlation coefficients were calculated between each feature and mRNA expression values. Genes within the top 10% correlation range were selected for downstream

analysis. Significantly correlated genes were subjected to Gene Ontology Biological Process (GO-BP) enrichment analysis using the Cluster Profiler R package. Overrepresented pathways were identified, and false discovery rate (FDR) correction was applied. Enriched GO terms with FDR-adjusted $p < 0.05$ were considered statistically significant.

4. Results

4.1. Patient Cohorts and Survival

A total of 447 HNSC cases from TCGA-HNSC and 142 cases from CPTAC-HNSC were evaluated for overall survival. Among these patients, 208 TCGA-HNSC cases (46.5%) and 55 CPTAC-HNSC cases (38.7%) experienced death events during the study period. The mean follow-up duration (± standard deviation) was 936.3 ± 917.4 days in the TCGA-HNSC cohort and 925.5 ± 548.2 days in the CPTAC-HNSC cohort. A log-rank test revealed no statistically significant difference in survival distributions between these two cohorts ($p = 0.1446$) (Fig 1). Overall clinical features weres summarized in Table 1. Of the total participants, 490 samples from the TCGA dataset and 94 samples from the HNSCC dataset had corresponding RNA expression data, making them eligible for downstream molecular analyses.

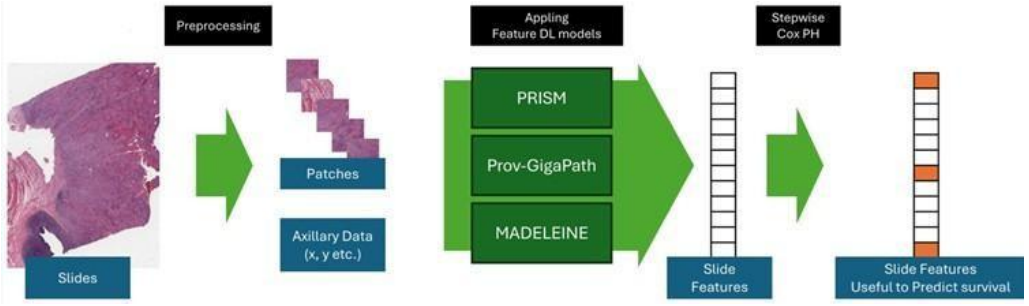

Figure 1: Overall workflow of the study.

Table 1: Summary of TCGA and CPTAC cohorts

	(Total (n=596	(CPTAC (n=146	(TCGA (n=450	*P value
(Age (years	(n=595)	(n=146)	(n=449)	0.961
	(11.3) 61.1	(9.0) 61.2	(12.0) 61.1	
(Lymph Nodes (n	(n=376)	NA	(n=376)	NA
	(22.3) 35.8		(22.3) 35.8	
(Lymph Nodes by H&E (n	(n=361)	NA	(n=361)	NA
	(4.4) 2.2		(4.4) 2.2	
(Overall Survival (days	(n=589)	(n=142)	(n=447)	0.894
	(843.0) 933.7	(548.2) 925.5	(917.5) 936.3	
Gender	(n=596)	(n=146)	(n=450)	
female	(23.3%) 139	(11.6%) 17	(27.1%) 122	0.001<
male	(76.7%) 457	(88.4%) 129	(72.9%) 328	
Death	(n=593)	(n=143)	(n=450)	
Occured	(44.7%) 265	(% 39.2) 56	(% 46.4) 209	0.153
Not occured	(55.3%) 328	(% 60.8) 87	(% 53.6) 241	
T Stage	(n=554)	(n=146)	(n=408)	
1	(% 9.2) 51	(% 7.5) 11	(% 9.8) 40	
2	(% 32.9) 182	(% 40.4) 59	(% 30.1) 123	0.06
3	(% 22.4) 124	(% 24.0) 35	(% 21.8) 89	
4	(% 35.6) 197	(% 28.1) 41	(% 38.2) 156	
N Stage	(n=552)	(n=118)	(n=434)	
0	(% 47.8) 264	(% 38.1) 45	(% 50.5) 219	
1	(% 14.1) 78	(% 20.3) 24	(% 12.4) 54	0.001<
2	(% 34.8) 192	(% 33.1) 39	(% 35.3) 153	
3	(% 3.3) 18	(% 8.5) 10	(% 1.8) 8	
M Stage	(n=562)	(n=137)	(n=425)	
0	(% 98.9) 556	(% 100.0) 137	(% 98.6) 419	0.357
1	(% 1.1) 6	(% 0.0) 0	(% 1.4) 6	

Clinical Stage	(n=549)	(n=146)	(n=403)	
1	(% 5.6) 31	(% 6.2) 9	(% 5.5) 22	
2	(% 18.4) 101	(% 21.2) 31	(% 17.4) 70	0.036
3	(% 20.2) 111	(% 26.7) 39	(% 17.9) 72	
4	(% 55.7) 306	(% 45.9) 67	(% 59.3) 239	
Primary LN Presence	(n=423)		(n=423)	
0	(% 10.6) 45	NA	(% 10.6) 45	NA
1	(% 89.4) 378		(% 89.4) 378	
Tumor Grade	(n=581)	(n=146)	(n=435)	
1	(% 14.1) 82	(% 17.8) 26	(% 12.9) 56	
2	(% 63.2) 367	(% 69.9) 102	(% 60.9) 265	0.004
3	(% 21.5) 125	(% 12.3) 18	(% 24.6) 107	
4	(% 1.2) 7	(% 0.0) 0	(% 100.0) 7	
Smoking History	(n=436)		(n=436)	
Non-smoker	(% 37.4) 163	NA	(% 37.4) 163	NA
Ex-smoker	(% 27.5) 120		(% 27.5) 120	
Current smoker	(% 35.1) 153		(% 35.1) 153	
Margin Status	(n=410)		(n=410)	
Close	(% 12.0) 49	NA	(% 12.0) 49	NA
Negative	(% 74.9) 307		(% 74.9) 307	
Positive	(% 13.2) 54		(% 13.2) 54	
Perineural Invasion	(n=324)		(n=324)	
No	(% 52.5) 170	NA	(% 52.5) 170	NA
Yes	(% 47.5) 154		(% 47.5) 154	
Lymphovascular Invasion	(n=317)		(n=317)	
No	(% 64.7) 205	NA	(% 64.7) 205	NA
Yes	(% 35.3) 112		(% 35.3) 112	
Alcohol History	(n=439)		(n=439)	
No	(% 34.2) 150	NA	(% 34.2) 150	NA
Yes	(% 65.8) 289		(% 65.8) 289	
Lymphnode Neck Dissection	(n=448)		(n=448)	
No	(% 15.8) 71	NA	(% 15.8) 71	NA
Yes	(% 84.2) 377		(% 84.2) 377	
Pathological Nodal Extracapsular Spread	(n=333)		(n=333)	
No Extranodal Extension	(% 67.3) 224	NA	(% 67.3) 224	NA
Microscopic Extension	(% 21.6) 72		(% 21.6) 72	
Gross Extension	(% 11.1) 37		(% 11.1) 37	

P value is t-test or Chi-square test*

4.2. Foundation Features and Survival Analysis Using Multiple Methods

Each feature slide extraction model's detailed was summarized in Table 2. All extracted features were stored in a structured format for subsequent statistical and bioinformatics analyses (Appendix 1).

From the stepwise variable selection for a Cox proportional hazards were runned in all foundation features, PRISM identified 116 features (9.1%) that were significantly associated with survival, while Prov-Giga Path identified 31 features (4.0%) and MADELEINE 38 features (7.4%) in TCGAdataset. In the CPTAC dataset, PRISM identified 400 (31.3%) significant features, Prov-Giga Path identified 168 (21.9%), and MADELEINE identified 159 (31.1%). Best cutoff figures in both cohort groups and features were showen in Figure 2. Of those significant features, 701 (54.8%) for PRISM, 379 (49.3%) features for Prov-Giga Path and 289 (56.4%) for MADELEINE were significant in both datasets. To further explore the molecular correlates of these survival-associated features, the study assessed the proportion of mRNAs with absolute Spearman correlation coefficients above 0.3. In the CPTAC dataset, 1.64% of PRISM extracted features, 2.09% of Prov-Giga Path extracted features and 0.89% of

MADELEINE extracted features met this criterion. By contrast, these percentages were lower in the TCGA dataset, at 0.28% for PRISM 0.003% for Prov-Giga Path and 0.08% for MADELEINE. Several genes appeared repeatedly among the most strongly correlated features. For example, in the TCGA dataset, Giga path identified PXYLP1, DIPK2A, MYB, CCDC150, and GLS2 as notably correlated, while in the CPTAC dataset, BCL10, RLF, KLHL2P1, ZBTB16, and ARHGEF1 emerged. Similarly, in Madeleine, the most correlated genes in the TCGA dataset were CCDC150, TNFRSF12A, AREG, ARSI, and PXYLP1, whereas in the CPTAC dataset, MAPK6, FAM83A-AS1, DUOX1, JUP, and BCL2L2 were highlighted. PRISM's most prominent correlations in the TCGA dataset included GLS2, KRT14, ACTN1, LOC730101, and PXYLP1, and in the CPTAC dataset, S100A8, SFN, KRT6A, TENT5B, and KRT6B were especially relevant. Gene Ontology (GO) enrichment analyses were also conducted on the identified features. Of the survival-associated features, 249 (35.5%) from PRISM, 77 (26.6%) from Prov-Giga Path, and 19 (5.0%) from MADELEINE mapped to at least one enriched GO term. PRISM's analyses highlighted the importance of epidermis development, whereas Prov-Giga Path showed strong enrichment for epidermal cell differentiation, epidermis development, intermediate filament organization, and keratinocyte differentiation. In contrast, skin development emerged prominently from MADELEINE results. On average, each survival-significant feature was annotated with 49.0 GO terms in PRISM, 40.6 in Prov-Giga Path, and 28.1 in MADELEINE. Of the 6193 GO terms investigated, 46 GO terms common to all three methods, and 1677 terms were shown at least one of the models.

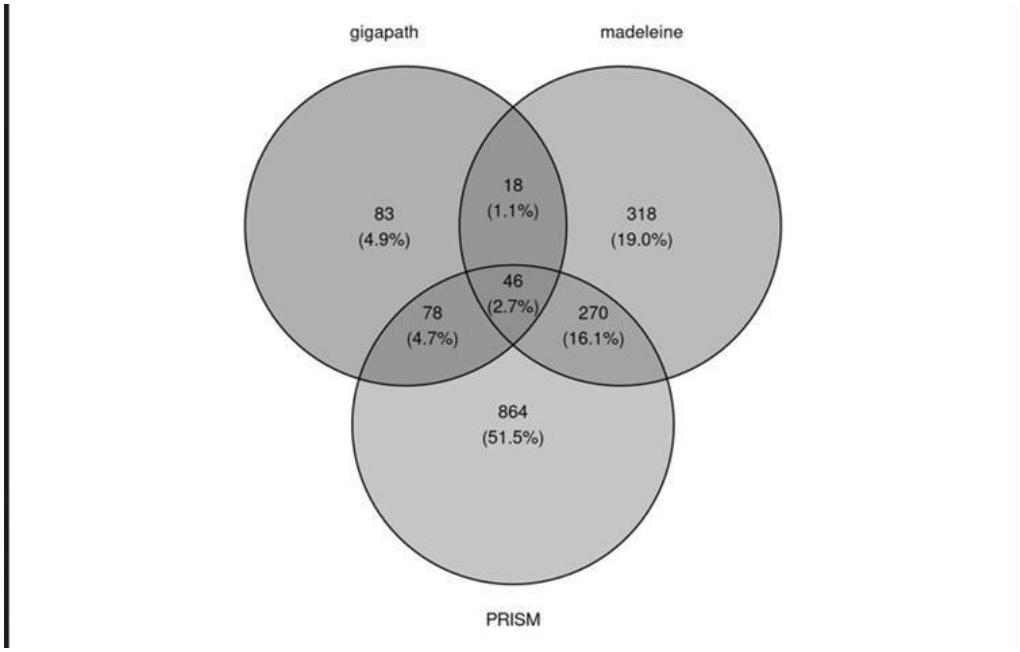

.**Figure 2:** Venn Diagram for GO-BP Terms in Each Foundation Group

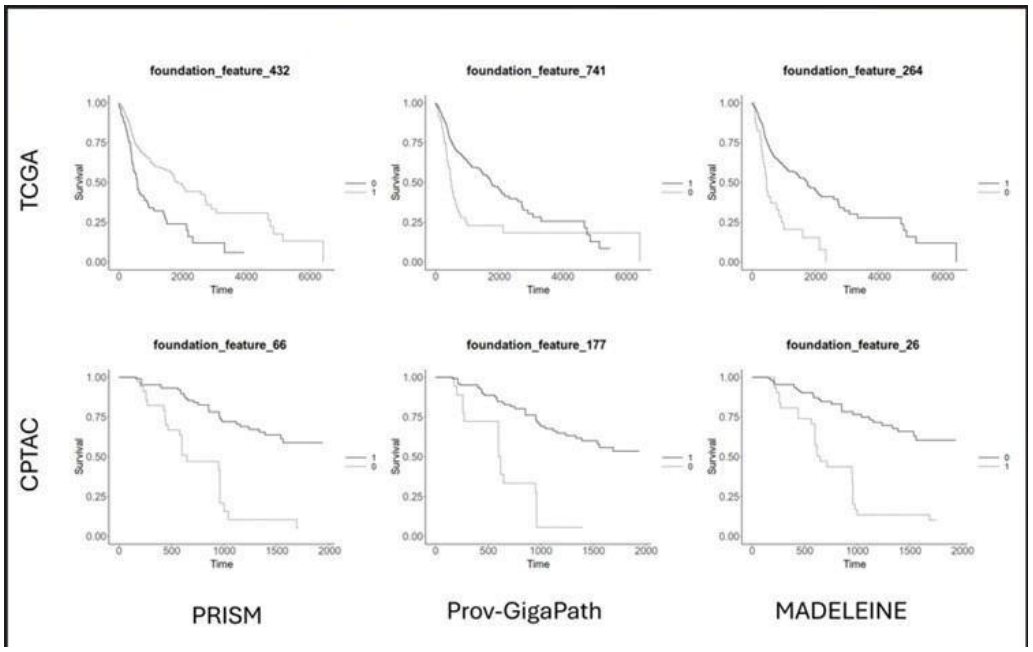

Figure 3: Survival Plots for Top Statistically Significant Features in TCGA-HNSC and CPTAC-HNSC.

Table 2: Summary of slide foundtaion models

	Pixel size of Patches	Magnification of Patches	Number of slide Features	Etc
MADELEINE	x 224 224	10x	512	x, y needed
Prov-GigaPath	x 224 224	20x	768	
PRISM	x 256 256	10x	1280	

Table 3: Summary of statistically significant slide foundation features after stepwise selection in the Cox proportional hazards regression model is performed

	Both	TCGA* only	CPTAC† only
PRISM	(3.5%) 45	(5.5%) 71	(27.7%) 355
Prov-GigaPath	(0.7%) 5	(3.4%) 26	(21.2%) 163
MADELEINE	17	21	142

*The Cancer Genome Atlas

†Office of Cancer Clinical Proteomics Research

Table 4: Top 5 Key Features of High-Performing Pathology Foundation Models Based on C-Index Evaluation

PRISM		Prov-GigaPath		MADELEINE	
*TCGA	†CPTAC	*TCGA	†CPTAC	*TCGA	†CPTAC
0.72	0.735	0.719	0.742	0.716	0.731
0.716	0.735	0.716	0.725	0.714	0.719
0.716	0.733	0.716	0.722	0.713	0.709
0.715	0.73	0.713	0.719	0.713	0.707
0.713	0.729	0.713	0.718	0.712	0.704

*The Cancer Genome Atlas

†Office of Cancer Clinical Proteomics Research

Table 5: five GO terms of best common p-value's features in pathology foundtaion model from TCGA(The Cancer Genome Atlas) and CPTA-C(Office of Cancer Clinical Proteomics) Research

Model	ID	Description	p.adjust
PRISM	GO:0031424	Keratinization	1.72E-04
	GO:0008544	epidermis development	6.91E-04
	GO:0000725	recombinational repair	1.37E-03
	GO:0006275	regulation of DNA replication	1.37E-03
	GO:0000724	double-strand break repair via homologous recombination	1.37E-03
Prov-GigaPath	GO:0006260	DNA replication	2.80E-07
	GO:0006261	DNA-templated DNA replication	1.03E-06
	GO:0006302	double-strand break repair	4.46E-06
	GO:0090329	regulation of DNA-templated DNA replication	7.64E-06
	GO:0036297	interstrand cross-link repair	1.42E-05
MADELEINE	GO:0006302	double-strand break repair	4.24E-05
	GO:2000779	regulation of double-strand break repair	3.59E-04
	GO:0006282	regulation of DNA repair	1.24E-03
	GO:2000781	positive regulation of double-strand break repair	6.62E-03
	GO:0045739	positive regulation of DNA repair	6.62E-03

5. Discussion

development and are expected to become an integral part of ongoing advances in digital diagnostics [20,21]. The emergence of pathology foundation models represents a paradigm shift in the field of digital pathology and AI-assisted diagnostics. This study investigated survival-related features in head and neck squamous cell carcinoma (HNSC) by integrating data from two large consortia (TCGA and CPTAC) and applying multiple slide feature extraction models (PRISM, Prov-Giga Path, and MADELEINE). The analysis to find significant revealed a range of image-derived features that correlated with clinical outcomes. Additionally, several features were found to be significantly associated with mRNA expression patterns, suggesting potential molecular underpinnings for the observed prognostic signals. One notable finding was the broad number of features identified as survival-associated within individual datasets. While this may indicate the presence of true biological heterogeneity, it could also reflect the varying sensitivities of different computational pipelines. Models such as PRISM, for example, identified a relatively high proportion of significant features, whereas Madeleine found fewer but still meaningful associations. This discrepancy underscores the potential value of applying multiple analytic methods to large-scale histopathology datasets: each model leverages distinct architectures and training strategies, capturing unique aspects of tumor morphology. Further support for the morphological and molecular complexity of HNSC emerged from the correlation analysis, which showed that certain genes consistently appeared as top correlates with slide features. The identification of genes involved in structural integrity (e.g., keratin family members), immune regulation, and cell signaling pathways suggests that both the composition of the tumor microenvironment and the intrinsic characteristics of cancer cells shape disease progression. Although the proportion of mRNAs that reached a high correlation threshold varied between the CPTAC and TCGA datasets, recurring themes across cohorts point to common molecular processes, such as epithelial differentiation and the regulation of inflammatory pathways. The Gene Ontology (GO) enrichment further illuminated these processes. In particular, enriched terms relating to epidermal cell differentiation, keratinocyte development, and intermediate filament organization align with the well-known disruption of epithelial architecture in HNSC. The variation in the number of annotated GO terms across PRISM, Giga path, and Madeleine highlights how different computational frameworks may emphasize distinct facets of tumor biology, even as they converge on certain core processes. One key observation is that although survival distributions did not differ significantly between TCGA and HNSCC, substantial heterogeneity in gene expression signatures was still evident. This might reflect the extensive genomic and clinical complexity typical of head and neck cancers, which are influenced by an array of factors including environmental exposures (e.g., tobacco, alcohol), human papillomavirus (HPV) status, anatomical site differences, and treatment modalities [22,23]. The moderate to high percentages of significant gene features identified within each method underscore the complexity of HNSCC, where multiple pathways likely drive tumor progression and influence prognosis. Despite the lack of inter-cohort survival differences, considerable heterogeneity emerged in gene expression signatures. This heterogeneity is consistent with the multifactorial nature of HNSC pathogenesis and progression. Many tumor-associated pathways likely operate simultaneously, driving invasive behavior, metastatic potential, and therapy resistance. In line with this, our multi-method approach (Giga path, Madeleine, PRISM) identified overlapping yet distinct sets of survival-associated features and correlated genes. Such variability highlights the value of employing multiple analytic strategies to capture the breadth of molecular diversity in HNSC. Among the identified genes, several stood out for their established or emerging roles in cancer. For example, BCL10 is known to be involved in NF-κB signaling and has been implicated in various lymphoid malignancies, though its potential role in epithelial tumors is less well-characterized.(24) MYB, classically considered a proto-oncogene in hematological malignancies, may also modulate proliferation and differentiation in solid tumors [25]. JUP (junction plakoglobin) and keratin family members such as KRT6B and KRT14 participate in maintaining epithelial integrity; dysregulation of these genes could contribute to the invasive phenotype characteristic of HNSC [26]. Their recurrent appearance across multiple analytical approaches and datasets strengthens the hypothesis that alterations in structural and cell-adhesion pathways underpin malignant transformation and progression in the head and neck region. Gene Ontology (GO) enrichment analyses offered additional discrapancy on these foundtaion models. PRISM frequently identified processes tied to epidermis development, whereas Gigapath emphasized keratinocyte migration and, in some cases, the positive regulation of proteasomal protein catabolic processes. Indeed, prior studies have implicated these pathways in HNSC pathogenesis, suggesting that proteostasis, epithelial integrity, and migration are central to tumor aggressiveness [27-29]. As each method also detected unique subsets of significant genes and GO terms, it suggested that integrating multiple analytic platforms may provide a more comprehensive understanding of the molecular heterogeneity present in HNSCC. From a clinical standpoint, the integration of imaging features, survival data, and transcriptomic profiles hints at potential strategies for more personalized care. Features that reliably distinguish high-risk from low-risk patients could be used to tailor treatment regimens, such as the intensity of surgery, radiation, or adjuvant therapies. Moreover, the recurrent associations with genes involved in structural and immune pathways raise the possibility of targeted interventions either in the form of novel small-molecule inhibitors or immunomodulatory agents. Despite these promising insights, several challenges remain. Although combining datasets can increase statistical power, it

also introduces variability stemming from differences in patient demographics, data acquisition procedures, and treatment protocols. tandardized quality control measures, multicenter validation, and larger patient cohorts are needed to confirm the robustness and generalizability of any candidate biomarkers identified. Additionally, a lack of uniform criteria for defining "best p-value cutoffs" may introduce biases in survival analyses, emphasizing the importance of reproducibility in future work. In conclusion, this study highlights the added value of leveraging large-scale digital pathology images, multiple computational feature-extraction pipelines, and transcriptomic data to advance our understanding of HNSC. The results suggest that morphological features captured by deep learning models can uncover biologically relevant signals tied to patient outcomes, and that these signals often converge on pathways linked to epithelial structure and inflammation. Future studies incorporating multi-omic approaches and prospective clinical validation will be critical to translating these computational findings into actionable strategies that can improve prognosis and treatment selection in head and neck oncology.

6. Conclusion

Pathologic Foundation models in HNSC could identify morphological features which are statistically significant with overall survials and might be tied to critical molecular pathways, potentially guiding personalized treatment strategies. Though variations in model's features persist, these approaches could be one way for significantly enhancing patient care through earlier and more accurate diagnostics, paving the way for larger multimodal HNSC studies.

7. Acknowledgments

This work was supported by the new faculty startup fund from Seoul National University (860 20210108 and this work supported by the national research foundation of Korea (NRF) grant funded by the Korean government (MSIP) 2020R1C1C1003834).

References

1. Bray F, Laversanne M, Sung H, Ferlay J, Siegel RL. Global cancer statistics 2022: GLOBOCAN estimates of incidence and mortality worldwide for 36 cancers in 185 countries. CA: a cancer journal for clinicians. 2024; 74(3): 229-63.
2. Ang KK, Harris J, Wheeler R. Schache A. Human Papillomavirus and Survival of Patients with Oropharyngeal Cancer. N Engl J Med. 2010; 363: 24–35. 50 Landmark Papers every Oral and Maxillofacial Surgeon Should Know: CRC Press. 2020; 31-6.
3. Dave M, Hunter K. Updates from the 5th edition of the World Health Organisation Classification of head and neck tumours. SPRINGERNATURE CAMPUS, 4 CRINAN ST, LONDON, N1 9XW, ENGLAND. 2022; 79-80.
4. Leemans CR, Braakhuis BJ, Brakenhoff RH. The molecular biology of head and neck cancer. Nature reviews cancer. 2011; 11(1): 9-22.
5. Ang KK, Harris J, Wheeler R, Weber R, Rosenthal DI, Nguyen-Tân PF. Human papillomavirus and survival of patients with oropharyngeal cancer. New England Journal of Medicine. 2010; 363(1): 24-35.
6. Krizhevsky A, Sutskever I, Hinton GE. Imagenet classification with deep convolutional neural networks. Advances in neural information processing systems. 2012; 25.
7. Litjens G, Kooi T, Bejnordi BE, Setio AAA, Ciompi F. A survey on deep learning in medical image analysis. Medical image analysis. 2017; 42: 60-88.
8. Wang D, Khosla A, Gargeya R, Irshad H, Beck AH. Deep learning for identifying metastatic breast cancer. arXiv preprint arXiv:160605718. 2016.
9. Shen D, Wu G, Suk H-I. Deep learning in medical image analysis. Annual review of biomedical engineering. 2017; 19(1): 221-48.
10. Campanella G, Hanna MG, Geneslaw L, Miraflor A, Werneck Krauss Silva V. Clinical-grade computational pathology using weakly supervised deep learning on whole slide images. Nature medicine. 2019; 25(8): 1301-9.
11. Bejnordi BE, Veta M, Van Diest PJ, Van Ginneken B, Karssemeijer N. Diagnostic assessment of deep learning algorithms for detection of lymph node metastases in women with breast cancer. Jama. 2017; 318(22): 2199-210.
12. Steiner DF, MacDonald R, Liu Y, Truszkowski P, Hipp JD, Gammage C. Impact of deep learning assistance on the histopathologic review of lymph nodes for metastatic breast cancer. The American journal of surgical pathology. 2018; 42(12): 1636-46.
13. Schmitd L, Scanlon C, D'silva N. Perineural invasion in head and neck cancer. Journal of dental research. 2018; 97(7): 742-50.
14. Mandal R, Şenbabaoğlu Y, Desrichard A, Havel JJ, Dalin MG. The head and neck cancer immune landscape and its immunotherapeutic implications. JCI insight. 2016; 1(17).
15. Zhou S, Zheng J, Zhai W, Chen Y. Spatio-temporal heterogeneity in cancer evolution and tumor microenvironment of renal cell carcinoma with tumor thrombus. Cancer Letters. 2023: 216350.
16. Shaikovski G, Casson A, Severson K, Zimmermann E, Wang YK. PRISM: A Multi-Modal Generative Foundation Model for Slide-Level Histopathology. arXiv preprint arXiv:240510254. 2024.
17. Xu H, Usuyama N, Bagga J, Zhang S, Rao R, Naumann T, et al. A whole-slide foundation model for digital pathology from real-world data. Nature. 2024:1–8.
18. Jaume G, Vaidya A, Zhang A, H. Song A, J. Chen R. editors. Multistain pretraining for slide representation learning in pathology. European Conference on Computer Vision. 2024.
19. Mazumdar M, Glassman JR. Categorizing a prognostic variable: review of methods, code for easy implementation and applications to decision-making about cancer treatments. Statistics in medicine. 2000; 19(1): 113-32.
20. Mahesh N, Devishamani CS, Raghu K, Mahalingam M, Bysani P. Advancing healthcare: the role and impact of AI and foundation models. American Journal of Translational Research. 2024; 16(6): 2166.

21. Moor M, Banerjee O, Abad ZSH, Krumholz HM, Leskovec J, Topol EJ. Foundation models for generalist medical artificial intelligence. Nature. 2023; 616(7956): 259-65.
22. Network CGA. Comprehensive genomic characterization of head and neck squamous cell carcinomas. Nature. 2015; 517(7536): 576.
23. Leemans CR, Snijders PJ, Brakenhoff RH. The molecular landscape of head and neck cancer. Nature Reviews Cancer. 2018; 18(5): 269-82.
24. Willis TG, Jadayel DM, Du M-Q, Peng H, Perry AR, Abdul-Rauf M. Bcl10 is involved in t (1; 14) (p22; q32) of MALT B cell lymphoma and mutated in multiple tumor types. Cell. 1999; 96(1): 35-45.
25. Joaquin á, Watson R. Cell cycle regulation by the B-Myb transcription factor. Cellular and Molecular Life Sciences CMLS. 2003; 60: 2389-401.
26. Zhi X, Lamperska K, Golusinski P, Schork NJ, Luczewski L. Gene expression analysis of head and neck squamous cell carcinoma survival and recurrence. Oncotarget. 2014; 6(1): 547.
27. Wang J, Li J, Zhang L, Qin Y, Zhang F, Hu R. Comprehensive analysis of ubiquitin-proteasome system genes related to prognosis and immunosuppression in head and neck squamous cell carcinoma. Aging (albany NY). 2021; 13(16): 20277.
28. Danella EB, Costa De Medeiros M, D'Silva NJ. Cancer-associated keratinocytes: new members of the microenvironment in head and neck cancer. Molecular & Cellular Oncology. 2021; 8(4): 1933329.
29. Dudás J, Dietl W, Romani A, Reinold S, Glueckert R. Nerve growth factor (NGF)-Receptor survival axis in head and neck squamous cell carcinoma. International journal of molecular sciences. 2018; 19(6): 1771.